

# Stiff Macromolecules with Aliphatic Side Chains: Side Chain Mobility, Conformation, and Organization from 2D Solid-State NMR Spectroscopy

J. Clauss, K. Schmidt-Rohr, A. Adam, C. Boeffel, and H. W. Spiess\*

Max-Planck-Institut für Polymerforschung, Postfach 3148, D-6500 Mainz, Germany

Received March 3, 1992

**ABSTRACT:** Stiff macromolecules with flexible side chains are investigated by proton spin diffusion experiments with  $^{13}\text{C}$  detection and by a recently developed  $^1\text{H}$  wide-line separation 2D  $^1\text{H}$ - $^{13}\text{C}$  NMR experiment (WISE-NMR spectroscopy). The conformational order and the molecular mobility of the alkyl side chains ( $\text{C}_{16}\text{H}_{33}$ ) are characterized for samples with polyester, polyamide, and polyimide main chains. The side chains, which are phase-separated from the main chain in a layer-type structure, can form crystalline as well as amorphous phases. The sizes of these domains depend on the nature of the main chains and their organization. In the polyimide and the polyester with regular main-chain packing, crystalline as well as amorphous regions are observed extending over more than one layer spacing. The heterogeneity observed in the polyamide is only of the order of the layer spacing. The polyester can also be obtained in a modification with uniformly ordered but anisotropically mobile side chains and conformationally disordered main chains. These results indicate coupling between the main-chain and side-chain packing in the investigated stiff macromolecules with flexible side chains.

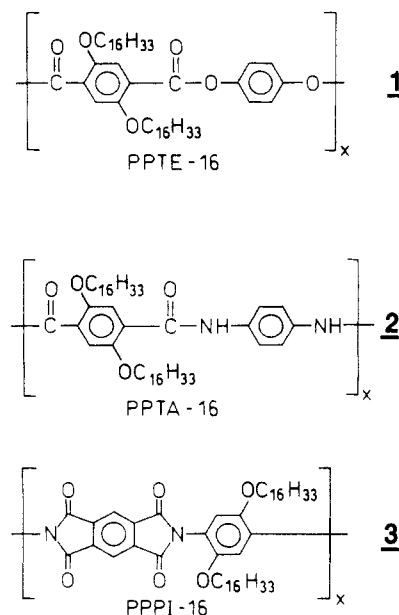
## Introduction

Stiff macromolecules have attracted considerable interest because of their unusual mechanical properties.<sup>1</sup> Para-substituted aromatic compounds in the polymer main chain, such as in poly(*p*-phenyleneterephthalamide) (PPTA), poly(*p*-phenylene terephthalate) (PPTE), and poly(*p*-phenylenepyromellitimide) (PPPI), exhibit extended rodlike chain structures. The highly anisotropic structure of the molecules results in a parallel packing of the chains and is responsible for the high modulus of fibers consisting of such polymers.<sup>1</sup>

The processing of these materials is difficult. Due to the chain stiffness the materials are virtually insoluble and do not melt. Several concepts for lowering the melting transitions and increasing the solubility of stiff macromolecules have been proposed and followed over the years.<sup>2,3</sup> One of these consists in attaching flexible aliphatic side chains to the stiff backbone.<sup>3,4</sup> However, it is found that spatial separation occurs between the flexible non-polar side chains and the rigid aromatic cores leading to layer-type packing structures.<sup>5</sup> The physical characterization of these systems has been the subject of several investigations<sup>4</sup> using X-ray analysis,<sup>6</sup> solid-state NMR spectroscopy,<sup>7,8</sup> and small-angle neutron scattering (SANS).<sup>9,10</sup>

Solid-state NMR methods allow the investigation of local orientation, dynamics, and conformational order of polymer chain segments.<sup>11</sup>  $^{13}\text{C}$  chemical shifts contain information about molecular moieties and about the conformation of chain segments. The line width of a  $^1\text{H}$  wide-line spectrum characterizes the strength of the dipolar couplings among protons and, therefore, the molecular mobility.  $^1\text{H}$  spin diffusion, mediated by the homonuclear dipolar couplings, is a powerful technique to obtain information about the spatial proximity of molecular moieties. These concepts have recently been combined in a two-dimensional  $^1\text{H}$ - $^{13}\text{C}$  wide-line separation experiment (WISE-NMR spectroscopy).<sup>12</sup> In this paper, we present the results of applying WISE-NMR and proton spin diffusion experiments<sup>13</sup> to stiff macromolecules with flexible side chains. The WISE-NMR spectra demonstrate the existence of rigid and mobile side-chain domains and characterize them with respect to the predominant chain

**Scheme I**  
**Molecular Structures of the Investigated Systems**  
**PPTE-16, PPTA-16, and PPPI-16**



conformations and the local chain mobility. Proton spin diffusion experiments with  $^{13}\text{C}$  detection<sup>13</sup> are used to obtain morphological data, like the typical sizes of such domains.

Three different systems have been investigated: the polyester PPTE-16, the polyamide PPTA-16, and the polyimide PPPI-16 (Scheme I). The synthesis and characterization of the samples have been described elsewhere.<sup>4</sup> Two modifications are distinguished by different packing of the main chain<sup>14</sup> (see Figure 1: Ordered single layers with main-chain distances around 0.55 nm (B modification, semicrystalline) or less ordered zigzag sheets (A modification, semicrystalline or amorphous)). The side chains are arranged perpendicular to the layer planes in the A but tilted in the B modification. Therefore the layer spacings as determined by X-ray diffraction differ substantially,<sup>4</sup> i.e. 2.8 and 2.2 nm for A and B, respectively, and both modifications can easily be discriminated. All

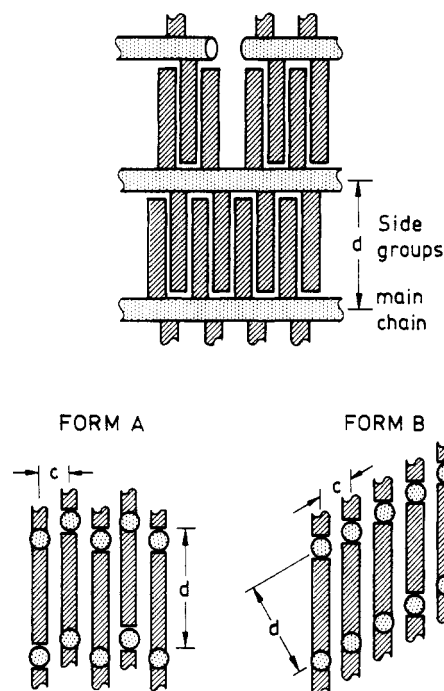


**Figure 1.** Packing model of stiff macromolecules with flexible side chains viewed along the backbones: zigzag sheets (modification A) and single layers (modification B).  $c$  and  $d$  denote the main-chain distance and the layer spacing, respectively.

measurements were performed at room temperature. Specifically, we studied PPTA-16 in its A modification, PPPI-16 in the B modification, and PPTE-16 in both the A and B modifications. The B modification of the polyester is metastable and can be obtained by treating the material with dioxane.<sup>15</sup>

## Experimental Part

**Wideline Separation 2D NMR Spectroscopy.** To facilitate understanding of the spectra, we summarize the relevant features of the recently developed two-dimensional experiment with  $^1\text{H}$  wideline separation (WISE-NMR spectroscopy) in a  $^{13}\text{C}$  MAS spectral coordinate.<sup>12</sup> The pulse sequence is shown in Figure 2a. During the preparation time, a  $90^\circ$  pulse to  $^{13}\text{C}$  destroys any  $^{13}\text{C}$  magnetization from highly mobile segments left over the previous scans. For simplification, this pulse is not shown in Figure 2a. After a  $90^\circ$  proton pulse, the proton magnetization evolves under the influence of dipolar coupling. Cross polarization transfers the proton magnetization to  $^{13}\text{C}$ , where it is detected after removing spinning sidebands with a TOSS (total suppression of spinning side bands) sequence.<sup>16</sup> Incrementing the proton evolution time  $t_1$  leads to a modulated  $^{13}\text{C}$  signal, and subsequent two-dimensional Fourier transformation yields a spectrum with dipolar-broadened proton lines resolved in  $t_2$  by the carbon spectrum. More details of the WISE-NMR experiment, in particular the introduction of spin diffusion, are described elsewhere.<sup>12</sup> In our experiments the  $90^\circ$  pulse width for the  $^1\text{H}$  and  $^{13}\text{C}$  pulses was  $3.5\ \mu\text{s}$ . The data matrix had a size of 128 points in the  $t_1$  ( $^1\text{H}$ ) dimension and 1024 complex data points in the  $t_2$  ( $^{13}\text{C}$ ) dimension. The spectral width in  $t_1$  was 200 kHz (dwell time  $5\ \mu\text{s}$ ) and 20 kHz in  $t_2$  (dwell time  $25\ \mu\text{s}$ ). The cross polarization time was  $300\ \mu\text{s}$ . Typically, 96 scans were taken for each slice with a repetition time of 3 s, resulting in a measuring time of ca. 10 h for one 2D spectrum.

**Spin Diffusion Experiments.** The spin diffusion experiments were carried out using the selection of proton magnetization in mobile domains by the "dipolar filter" pulse sequence shown in Figure 2b.<sup>17</sup>

All NMR experiments were performed on a Bruker MSL300 spectrometer at a  $^1\text{H}$  frequency of 300.13 MHz and a  $^{13}\text{C}$  frequency of 75.47 MHz. The experiments were carried out using a double-bearing variable-temperature Bruker MAS probe and 7-mm zirconium oxide rotors at 300 K.

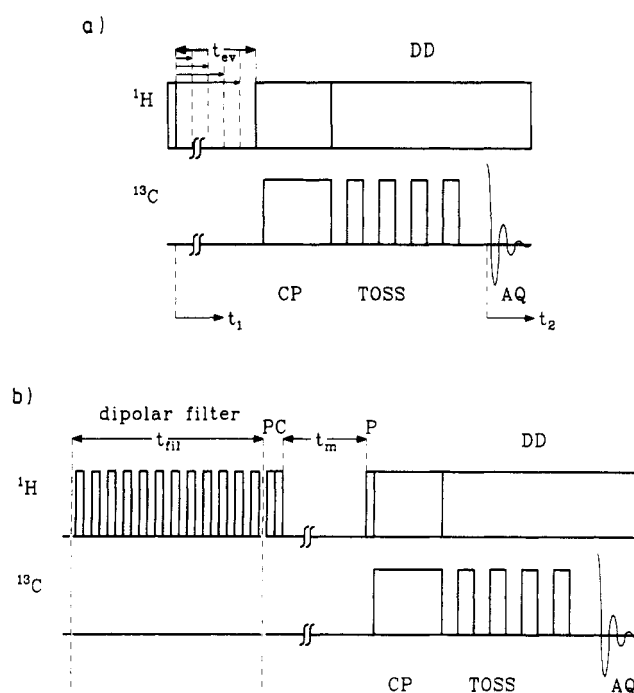


**Figure 2.** (a) Pulse sequence of the 2D WISE-NMR experiment: After a  $90^\circ$  pulse on the proton channel, the  $^1\text{H}$  magnetization evolves for a time  $t_1$ , which is incremented in the course of the experiment. By cross polarization (CP), proton magnetization is transferred to the carbon-13 nuclei nearby. After TOSS (total suppression of sidebands), the  $^{13}\text{C}$  signal is acquired under high-power decoupling (DD). (b) Pulse sequence for the selection of magnetization using the dipolar filter. The filter cycle consists of twelve  $90^\circ$  pulses of phases  $(x, -y, x, x, -y, x, -x, y, -x, -x, y, -x)$ . Usually several cycles are repeated. Before the mixing time  $t_m$ , a phase-cycled (PC) pulse flips the magnetization to  $(-z)$  in every other scan to eliminate artifacts from  $T_1$  relaxation. For CP and  $^{13}\text{C}$  detection, refer to the caption of (a).

## Results and Discussion

**Conformation and Mobility of the Side Chains.** Whereas in liquids the chemical shift is determined by the structure of the molecule, in the solid state it is also sensitive to the conformation and differences in packing. The sensitivity to the conformation for methylene units, the so-called  $\gamma$ -gauche effect,<sup>18</sup> has been extensively exploited in the characterization of  $n$ -alkanes, cycloalkanes, and polyethylenes.<sup>19</sup> The local field for methylene groups in alkyl chains depends on the conformations of the two  $\gamma$ -positions: gauche-gauche, trans-gauche/gauche-trans, or trans-trans. This leads to a low-field shift of approximately 4.5 ppm for a methylene unit in a trans-trans chain compared to one in a trans-gauche and approximately 9 ppm compared to one in a gauche-gauche environment. Dynamic averaging of trans and gauche states as found in fluid phases and far above the glass transition leads to correspondingly averaged values.

Polyethylene can be used for comparison for the aliphatic substituents in the stiff macromolecules with flexible side chains investigated. They are similar from the spectroscopic point of view, even though the binding of the side chains to the stiff main chain represents a restricting boundary condition. Therefore, a 2D WISE-NMR spectrum of low-density poly(ethylene), LDPE, is shown in Figure 3. The carbon spectrum exhibits two signals reflecting the amorphous regions with high gauche content around  $\delta_{^{13}\text{C}} = 30.8$  ppm (reference TMS) and the crystalline regions at  $\delta_{^{13}\text{C}} = 32.7$  ppm (inset Figure 3). The signal of the crystalline regions is narrow in the carbon dimension, reflecting the high degree of conformational order. In contrast, the signal of the amorphous parts is

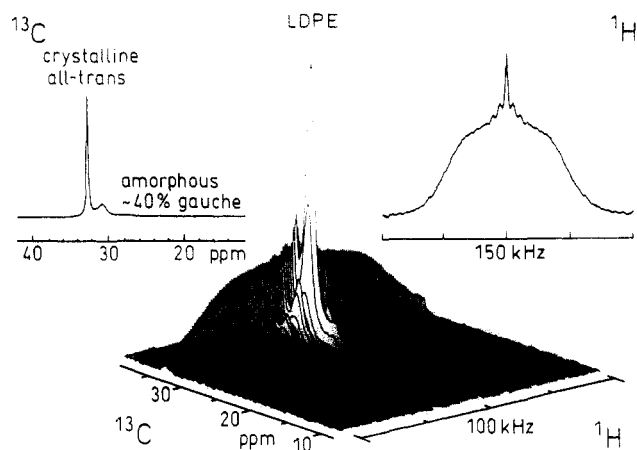


**Figure 3.** 2D WISE-NMR spectrum of low-density poly(ethylene) LDPE, the insets display the projection on the  $^{13}\text{C}$  dimension and the slice in the  $^1\text{H}$  dimension at  $\delta = 32.7$  ppm, corresponding to the all-trans chains in the crystalline regions.

**Table I**  
 $^{13}\text{C}$  Chemical Shifts for Transoid and Gauchoid Chain Segments, Their Distance  $\Delta\delta$  and Full Width at Half-Height  $\Delta\omega_{1/2}/2\pi$  of the  $^1\text{H}$  Line at the Position of the Transoid Chemical Shift ( $\delta_{\text{TC}}$ )

| system   | $\delta_{\text{TC}}(\text{t})$ , ppm | $\delta_{\text{TC}}(\text{g})$ , ppm | $\Delta\delta$ | $\Delta\omega_{1/2}/2\pi$ |
|----------|--------------------------------------|--------------------------------------|----------------|---------------------------|
| LDPE     | 32.7                                 | 30.8                                 | 1.9            | 75                        |
| PPPI-16  | 33.9                                 | 30.3                                 | 3.6            | 70                        |
| PPTE-16B | 33.7                                 | 30.4                                 | 3.3            | 70                        |
| PPTE-16A | 33.1                                 | 30.5                                 | 2.6            | 40                        |
| PPTA-16  | 33                                   | 31                                   | 2              | 40                        |

**Table II**  
Amount of Transoid and Gauchoid Chain Segments Derived from the Integrated Intensities of the Respective Signals (cf. Table I and Figures 4 and 5)<sup>a</sup>

| system | % $\delta_{\text{TC}}(\text{t})$ | % $\delta_{\text{TC}}(\text{g})$ | % gauche in t-signal | % gauche in g-signal | total content of gauche |
|--------|----------------------------------|----------------------------------|----------------------|----------------------|-------------------------|
| PPPI   | 51                               | 49                               | 0                    | 36                   | 18                      |
| PPTE-B | 63                               | 37                               | 2                    | 35                   | 15                      |
| PPTE-A | 82                               | 18                               | 8                    | 34                   | 13                      |
| PPTA   | 51                               | 49                               | 9                    | 29                   | 19                      |

<sup>a</sup> The values have been corrected for the different cross polarization efficiency. The amount of gauche conformations is given for the different regions.

broad in the carbon dimension due to the variations in the conformation and packing of the chains. The 2D WISE-NMR spectrum reveals the differences in mobility in the different surroundings from the  $^1\text{H}$  NMR line widths. The narrow line in the carbon dimension is broad in the  $^1\text{H}$  dimension due to large dipolar couplings resulting in a full line width at half-height of  $\Delta\omega_{1/2} \approx 75(2\pi)$  kHz. This reflects the immobility of the densely packed all-trans chains in the crystallites. The narrow  $^1\text{H}$  sidebands visible superposed on the broad line are due to an overlap with the amorphous signal. In contrast, the spectrum for the amorphous regions is rather narrow in the  $^1\text{H}$  dimension since there the dipolar coupling is almost averaged out by fast molecular motions, as is typical for amorphous polymers far above the glass transition. The small  $^{13}\text{C}$  high-field signals at 23 and 15 ppm in the 2D spectrum reflect methylene and methyl groups from side branches and chain ends concentrated in the amorphous regions. It should be noted that the signal intensities are weighted by the corresponding CP efficiencies. This typically favors rigid units with broad  $^1\text{H}$  lines (see also Table II).

As noted above the stiff macromolecules with flexible side chains differ among each other in their main-chain order and in the side-group packing. 2D WISE-NMR

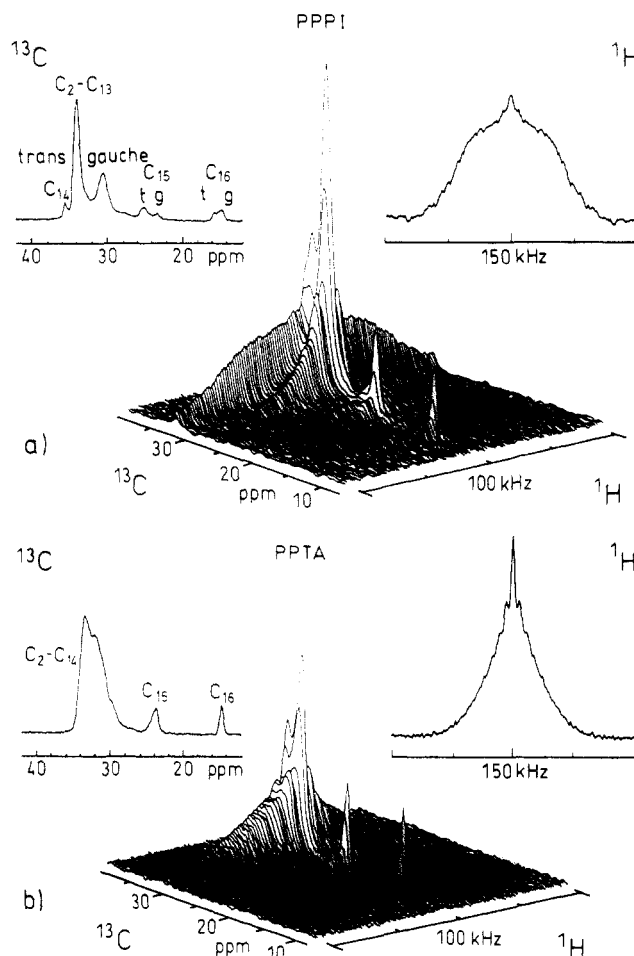


**Figure 4.** 2D WISE-NMR spectra of PPPI-16 (a) and PPTA-16 (b). For comparison the projections on the  $^{13}\text{C}$  axis and the  $^1\text{H}$  dimension at  $\delta = 33$  ppm are also shown in the insets.

spectra of the aliphatic region of the three systems are shown in Figures 4 and 5, giving a closer insight into the mobility and packing of the alkyl side chains in the different systems. In addition to the stacked plots, each figure contains insets showing the  $^{13}\text{C}$  MAS-NMR spectrum and the slice in the  $^1\text{H}$  dimension for the carbon positions 2 and 4–13 for extended trans segments at  $\delta \approx 33$  ppm (see also Figure 3). The polyimide PPPI-16 is only obtained in the B modification and exhibits a high X-ray crystallinity at room temperature.<sup>15,20</sup> Accordingly, the 2D WISE-NMR spectrum (Figure 4a) reveals a coexistence of two species: a rigid crystalline and a mobile amorphous side-chain region, with carbon chemical shifts of 33.9 and 30.3 ppm, respectively. The latter signal is narrow in the proton dimension and compared to LDPE the amorphous part is more heterogeneous in terms of mobility. The  $^1\text{H}$  line exhibits a pronounced broad component extending almost as far as that of the crystalline regions, presumably corresponding to carbons close to the stiff polymer chain. The signal of the crystalline regions at 33.9 ppm is broad in the proton dimension with  $\Delta\omega_{1/2} \approx 70(2\pi)$  kHz width at half-height and suggests an alkane-like monoclinic structure.<sup>21</sup>

Since the alkyl layers are separated by the main chain layers, the question arises whether the side-chain ends are incorporated in the crystallites. This can be checked by  $^{13}\text{C}$  and 2D WISE-NMR spectroscopy, because the signals of  $\text{C}_{15}$  and  $\text{C}_{16}$  are completely resolved. As seen from Figure 4a, a major part of the ends of the side chains ( $\text{C}_{15}$  and  $\text{C}_{16}$ ) are imbedded in the crystalline regions. In the  $^{13}\text{C}$  MAS spectrum the lines exhibit conformation-induced split-

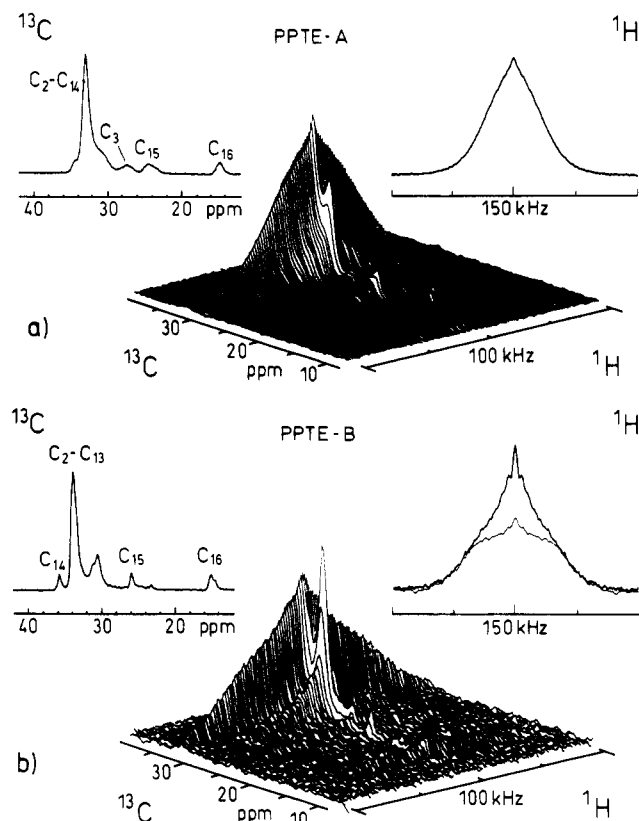


**Figure 5.** 2D WISE-NMR spectra of PPTE-16 in its two different modifications A (a) and B (b). For comparison, the projections of the  $^{13}\text{C}$  dimension and the  $^1\text{H}$  dimension at  $\delta = 33$  ppm are shown in the inset. The PPTE-16B contains about 25% of the A modification, as also determined by X-ray scattering. This is also obvious from the  $^1\text{H}$  NMR line shape. For this reason a scaled-down spectrum of PPPI-16 is reproduced in the same plot to illustrate that the PPTE-16B shows the same immobility. The narrow line on top of the spectrum has the same shape as the one shown in (a).

tings, and the large proton widths of the trans lines in the 2D WISE-NMR spectrum indicate immobilized chains. The splitting of the signal from amorphous and crystalline carbons in the central portion of the side chains in PPPI-16 amounts to 3.6 ppm and is thus almost twice as large as that of 1.9 ppm in LDPE. The mobility of large fractions of the amorphous material is more restricted than in LDPE, as indicated by the large  $^1\text{H}$  line width. This suggests smaller domain sizes than in LDPE caused by the neighborhood of the rigid main chains (see below).

A different behavior is shown by the polyamide PPTA-16 in its A modification (Figure 4b). This structure is stabilized by hydrogen bridges between the main chains.<sup>14</sup> Almost no splitting of the carbon signal due to extended and coiled chains can be detected. For  $\text{C}_2\text{-C}_{14}$  the spread of the chemical shifts is almost the same as in LDPE, with the high-field shoulder appearing close to 31 ppm and the low-field shoulder at 33 ppm. This shows that the methylene units experience a large conformational variety in the adjacent chain segments, but that no distinct phases are formed. This indicates a close spatial proximity of regions with extended and more coiled side chains, as is in fact confirmed by spin diffusion experiments reported in the next section. The proton line width of the more extended chain parts is significantly smaller than for LDPE and PPPI-16, with  $\Delta\omega_{1/2} \approx 40(2\pi)$  kHz. An intermediate mobility of a major portion of segments of both gaucheoid and transoid conformations is observed. In the  $^{13}\text{C}$  MAS spectrum the terminal methylene ( $\text{C}_{15}$ ) and methyl ( $\text{C}_{16}$ ) groups show no splitting. The  $^1\text{H}$  dimension of the 2D WISE-NMR spectrum, however, exhibits a superposition

of broad and narrow components, suggesting a heterogeneous packing with regions of different side-chain mobilities. Their sizes as determined by spin diffusion measurements will be discussed below.

For the polyester PPTE-16, the A modification is thermodynamically stable, but the material can also be obtained in the B modification by treatment with dioxane.<sup>15</sup> The 2D WISE-NMR spectra of both modifications are compared in Figure 5a,b. Almost no  $^{13}\text{C}$  signal due to gauche conformations is observed in the A modification. The signal from highly ordered trans segments is detected at 33.1 ppm with a small shoulder at 30.5 ppm. The high conformational order does not reflect a high rigidity, as seen from the relatively narrow lines in the proton dimension ( $\Delta\omega_{1/2} \approx 40(2\pi)$  kHz). This indicates higher chain mobility than in LDPE and PPPI-16. The dynamic process which reduces the line width considerably while at the same time retaining the extended-trans character of the chains must be a large-amplitude motion effective around the side-chain axes. The higher mobility of the aliphatic side chains in this system thus has to be linked to a looser packing. The behavior of the B modification is quite similar to PPPI-16, the trans signal is detected at 33.7 ppm with almost the same line width in the proton dimension as compared to PPPI-16 ( $\Delta\omega_{1/2} \approx 70(2\pi)$  kHz). The  $^1\text{H}$  line shape is actually a superposition of two species, since the material contains about 25% of the A modification, as known also from X-ray studies of this material.<sup>22</sup>

From the chemical shifts of the various  $\text{CH}_2$  units  $\text{C}_4\text{-C}_{13}$ , together with the mobility information from the 2D WISE-NMR spectra, some conclusions about the side-chain conformations can be drawn. The PPPI-16 side chains exhibit the most pronounced downfield shift (cf. Table I), indicating a very high trans content (Table II). Almost the same behavior is observed for PPTE-16B. The corresponding PPTA-16 and PPTE-16A side-chain signals are shifted by 0.8 and 0.9 ppm, respectively. With the mobility detected in the 2D WISE-NMR spectra, it is obvious that the chains cannot be in a well defined all-trans conformation. Therefore, a gauche content of 8 and 9% has to be considered in the ordered domains of these systems. The deviation of the chemical shift from the value expected for a chain in an extended trans conformation could also be attributed to torsions along the chain resulting from the anisotropic motion as detected from the partially averaged  $^1\text{H}$  line in the 2D WISE-NMR spectra. The similar chemical shifts of the gauche-rich environments of the different systems indicate that the amount of gauche conformers is comparable (for the detailed numbers, see Table II). The gauche contents obtained from  $^{13}\text{C}$  MAS-NMR spectra can be compared with molecular dynamic simulations of alkyl chains in stiff macromolecules with flexible side chains<sup>23</sup> and in model bilayer systems.<sup>24</sup> These analyses show that the amount of gauche conformers is strongly dependent on the free area per molecule; a decrease in density increases the gauche content. This is consistent with our observations that in the stiff macromolecules with flexible side chains no gauche conformers are present in the densely packed crystal regions whereas the loose packing of the amorphous areas allows for a higher amount of gauche conformations. The overall content of gauche conformations in PPTE-16A, as detected by NMR spectroscopy, is in agreement with the MD simulations.<sup>25</sup>

In summary, the results of the  $^{13}\text{C}$  MAS and the 2D WISE-NMR experiments reveal that the stiff macromolecules with flexible side chains exhibit different types of side-chain packing. The two B modifications are similar

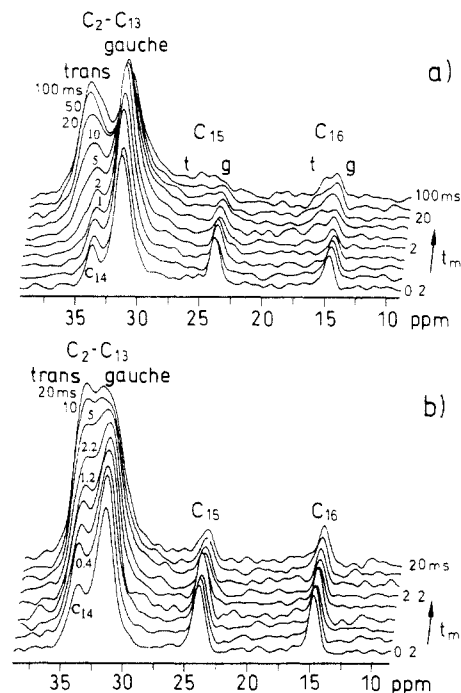


**Figure 6.** Spin diffusion experiments with  $^1\text{H}$  selection of the mobile regions and spin diffusion to the rigid regions ( $^{13}\text{C}$ -CP-MAS-TOSS detection): (a) PPPI-16; (b) PPTA-16. Note the different scales for the spin diffusion time for the two systems.

with a clear splitting of the  $^{13}\text{C}$  signal of the methylene units, reflecting heterogeneity of the structure in crystalline and amorphous regions. In the two A-type systems all carbons have more similar conformations. The  $^{13}\text{C}$  line width of the signal from the crystalline regions is broader than in LDPE, suggesting the lower conformational order in the alkyl side chains of the stiff macromolecules. In addition, this signal is shifted downfield as compared to LDPE, which crystallizes in an orthorhombic modification. For monoclinic alkane crystals and polyethylene modifications, chemical shifts of 34–35 ppm have been reported.<sup>21</sup> This fact suggests different packing structures of the alkyl side chains in the stiff macromolecules as compared to LDPE.<sup>6,26</sup> In the B modification, chain ends are incorporated into the crystalline regions. Likewise, the chain ends in the A modification exhibit different mobilities, suggesting the presence of spatially separated ordered and disordered regions which are considered in the following section.

**Domain Structure.** Spin diffusion experiments permit the investigation of the spatial separation between regions with mobile and rigid side chains, respectively. The selection of the magnetization of mobile units is achieved by means of the dipolar filter (see Experimental Part). The magnetization gradient continuously vanishes with time through spin diffusion, i.e. exchange of magnetization between the selected and nonselected protons. Polarization transfer to  $^{13}\text{C}$  is employed prior to detection because of the higher resolution in the carbon spectrum. Results of these experiments are plotted in Figure 6 for PPPI-16 and PPTA-16. For short mixing (spin diffusion) times, only the signals of the chain ends and the highly mobile amorphous parts are observed. This is similar to the  $^{13}\text{C}$  center slice at  $\omega_{\text{H}} = 0$  in the 2D WISE-NMR spectrum, see Figure 4. However, the carbon signals corresponding to broad  $^1\text{H}$  components are completely suppressed. For long mixing times, when spin diffusion is complete, the regular  $^{13}\text{C}$  MAS spectrum is obtained. In the polyamide a fast magnetization transfer to the more rigid regions is observed, i.e. exchange of magnetization is essentially

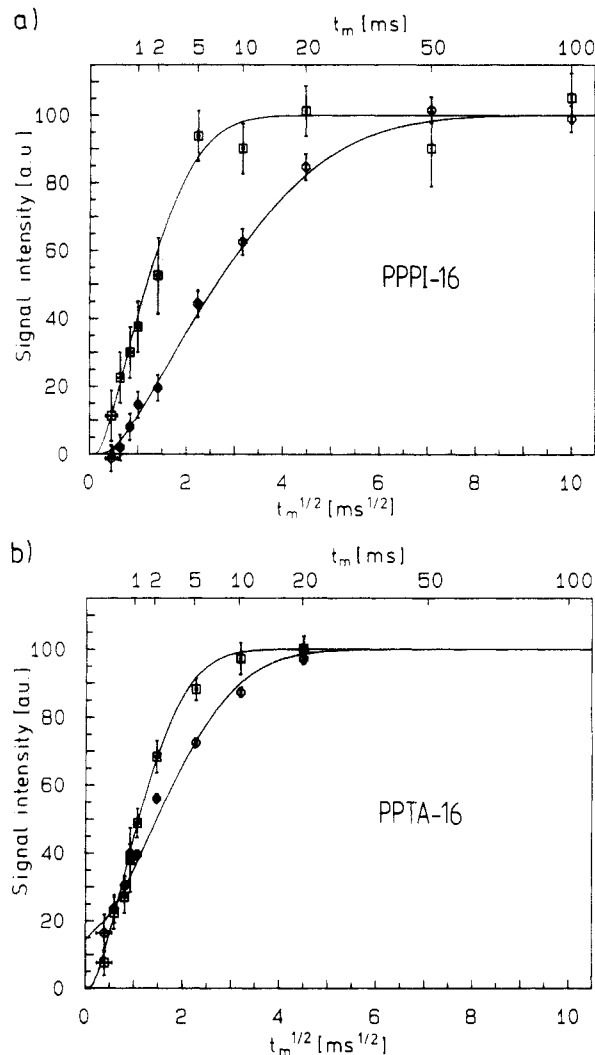


**Figure 7.** Signal intensity with spin diffusion from the mobile side chains to the aromatic main chains (□) and from the mobile to the rigid parts of the side chains (○): (a) PPPI-16; (b) PPTA-16.

complete after 10 ms. In contrast to this, in the polyimide the equilibrium is only reached after a mixing time of 100 ms (note the different scales in the mixing time for the two different systems). A plot of the increase of the signal intensity (Figure 7a,b) of the rigid parts (○) visualizes the difference of the two systems. The smallest typical diameters of the mobile parts are determined to be  $3.5 \pm 0.7$  nm in PPPI-16 and  $1.8 \pm 0.5$  nm in PPTA-16, respectively. The rigid regions have an extension of  $5.0 \pm 0.7$  nm for PPPI-16 and  $2.2 \pm 0.5$  nm for PPTA-16. The values of the diameters of the mobile parts include transition regions of  $0.5 \pm 0.2$  and  $0.2 \pm 0.2$  nm, respectively. Note that the given dimensions refer always to the smallest typical diameters. This results in domain sizes about twice as large as the layer spacing in PPPI-16, whereas they are of the order of the layer spacing in PPTA-16. Similar results as for PPPI-16 are obtained for PPTE-16B. The spin diffusion coefficient was calibrated with polyethylenes of known dimensions; the detailed values are summarized together with the fitted results in Table III. PPTE-16A was not investigated by this method, since the mobile units to be selected using the dipolar filter are present only in very low concentration (previous section, Figure 4a). The spin diffusion experiments thus fully confirm and quantify our analysis of the  $^{13}\text{C}$  MAS and 2D WISE-NMR spectra described in the previous section.

**Main-Chain Arrangement.** As noted already in the Introduction, the packing of the main chains is different

**Table III**  
Domain Sizes of the Two Systems PPPI-16 and PPTA-16 for Units of Different Mobility and Structure and the Spin Diffusion Coefficient Used in the Fits for the Determination of the Domain Sizes<sup>a</sup>

| packing unit        | PPPI-16   | PPTA-16   | <i>D</i> , nm <sup>2</sup> /ms |
|---------------------|-----------|-----------|--------------------------------|
| mobile side groups  | 3.5 ± 0.7 | 1.8 ± 0.5 | 0.05                           |
| interface           | 0.5 ± 0.2 | 0.5 ± 0.2 | 0.15                           |
| rigid side groups   | 5.0 ± 0.7 | 2.2 ± 0.5 | 0.7                            |
| aromatic main chain |           |           | 0.4                            |

<sup>a</sup> Note that the given dimensions refer to the smallest typical diameters.

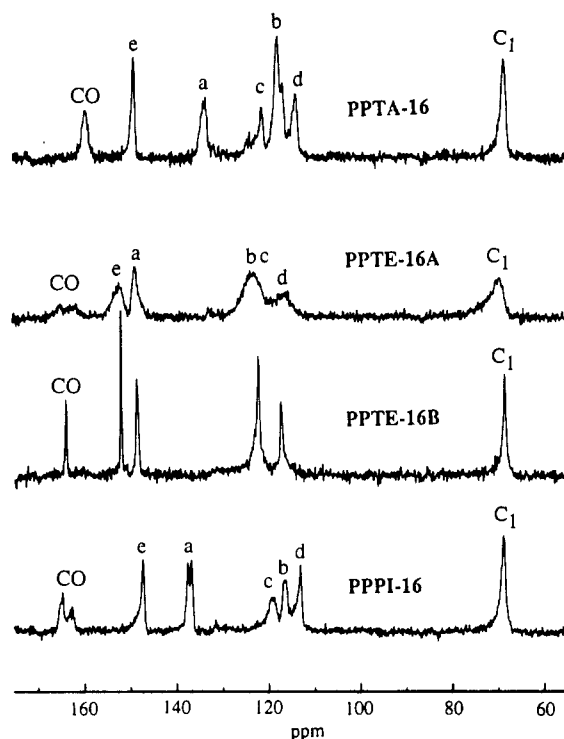
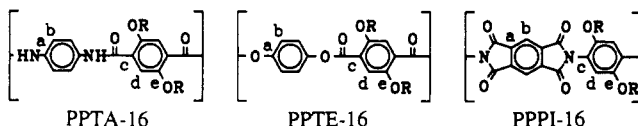


**Figure 8.** <sup>13</sup>C-CP-MAS TOSS spectra of the aromatic regions for the different stiff macromolecules with flexible side chains: PPTA-16, PPTE-16A, PPTE-16B, and PPPI-16 (from top to bottom). For assignment the chemical structures are shown on top of the figure.

in the two modifications, supposedly more ordered in the B and less ordered in the A modification.<sup>14</sup> In order to check this conjecture, <sup>13</sup>C MAS spectra for the aromatic and carbonyl chemical shift regions were recorded. Figure 8 presents the <sup>13</sup>C CP-MAS-TOSS spectra of the four systems in the range between 50 and 200 ppm. Indeed, the B-type systems exhibit sharp lines for the main-chain signals as well as for the α-methylene group. The carbon signals of the main chain and the α-methylene group in PPTE-16A are significantly broadened as compared to the other systems. In addition, a splitting of the carbonyl signal is observed, resulting from different local environments of the carbonyl group. The linkage between the terephthalic acid and the hydroquinone can be either trans or cis at the carbonyl and oxygen site, respectively.<sup>8</sup> The spectra for the two polyester modifications, in particular, reflect differences in packing and conformational order for the main chains. Note that PPTE-16B not only shows

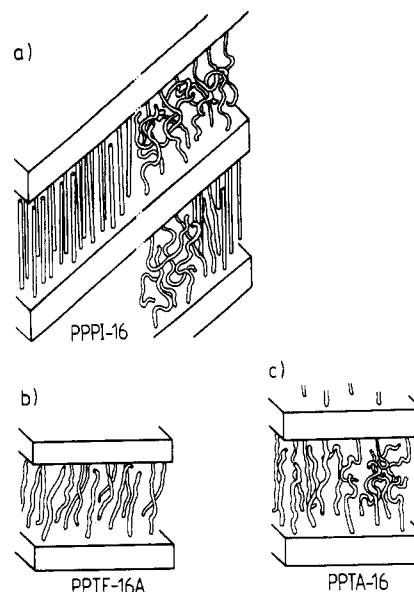


**Figure 9.** Schematic models illustrating the different morphologies in stiff macromolecules with flexible side chains. (a) B modifications of PPPI-16 and PPTA-16. The extension of crystalline and amorphous domains is larger than the layer spacing as indicated. (b) PPTE-16A. The chains are conformationally highly ordered but not crystallized. (c) PPTA-16. Conformationally ordered and disordered regions are in close proximity; the dimensions of both are smaller than the layer spacing.

narrow lines but also no splitting of the carbonyl lines. This suggests that in the B-modification the polyester main chain predominantly exists in the trans-trans conformation.

The <sup>13</sup>C lines of the polyamide, PPTA-16, are rather narrow, despite the packing in the A modification. Most likely this indicates a relatively ordered zigzag arrangement of the main chains, stabilized by hydrogen bonds between amide groups of neighboring chains as proposed in order to explain the packing behavior of these systems.<sup>14</sup> The signals for PPTA-16 are broadened as compared to the B modifications but the still relatively small <sup>13</sup>C line widths reflect a regular arrangement of the main chains due to the hydrogen bridges between amide groups of neighboring chains.

## Conclusion

The 2D WISE-NMR spectra and the spin diffusion results provide detailed information about the conformation, molecular dynamics, and spatial heterogeneities. This allows us to propose a picture of the packing behavior of the aliphatic groups in stiff macromolecules bearing flexible side chains, as displayed schematically in Figure 9. In the polyimide PPPI-16 and the polyester PPTE-16B, i.e. the systems with an arrangement of the main chains in a planar array, the side chains exhibit a considerable crystallinity (Figure 9a), with crystalline regions larger than the layer spacing. The chain ends are imbedded in these crystalline regions, as indicated from the splitting of their <sup>13</sup>C signals. At the same time amorphous regions of high mobility are detected; though, for considerable portions, rates or amplitudes of the corresponding motions are smaller than in LDPE. These findings with well-defined side-chain domains are reflected in the X-ray diffractograms<sup>14,20</sup> and in <sup>2</sup>H NMR data,<sup>26</sup> which also detect heterogeneities of the material.

A different situation is observed in the two A modifications, where the main chains form a staggered arrangement. The polyester exhibits extended side chains with low mobility. In addition to highly mobile gauche con-

formers, the polyamide shows segments of intermediate mobility for trans and gauche environments. The highly mobile regions extend over less than a layer spacing. Therefore we propose the structure in Figure 9b with essentially uniform extended side chains for the polyester and the structure in Figure 9c with spatially separated more extended and more disordered side chains, respectively, for the polyamide. The high uniformity of the polyester is not due to crystallinity of the side chains. X-ray studies indicate a disordered hexagonal packing.<sup>6</sup> Uniform anisotropic mobility of the side chains is detected in the 2D WISE-NMR spectra as described above, and <sup>2</sup>H NMR spectra also show a high uniform mobility of the different methylene positions along the side chains.<sup>26</sup> Together, these data suggest a relatively loose columnar structure of the side chains with no axial register between the chains.

Apparently, the main-chain ordering and the side-chain packing are closely connected. The regular arrangement of main chains in the B modification allows a restricted crystallization of the side chains. The limited size of the crystallites may indicate an incomplete commensurability of side-chain substitution positions along the main chains and favorable crystalline side-chain arrangements. The regular packing of the main chains in the B modification also requires a regular conformational order along the chain, as suggested by the <sup>13</sup>C MAS-NMR spectra for both the polyimide PPPI-16 and the polyester PPTE-16B. In the A modification, however, the staggered arrangement of the main chains apparently leads to side-chain distances that do not allow crystallization. The conformational order of the main chains in the polyester PPTE-16A is low whereas the side-chain structure is homogeneous. The higher conformational order of the main chain in the polyamide PPTA-16 is attributed to the stabilization of the structure through hydrogen bonding. This also explains the existence of only one modification, since the staggered arrangement allows for higher saturation of hydrogen bonding.<sup>15,26</sup>

The delicate balance between the organization of the incompatible rigid main chains and flexible side chains in their respective layers thus leads to a considerable variety in the packing of these interesting polymers with supramolecular structure. Our study demonstrates that advanced NMR techniques yield specific information supplementing computer-aided X-ray studies of such partially ordered systems<sup>27</sup> since NMR spectroscopy is sensitive to conformation, mobility, and spatial proximity of different structural elements.

**Acknowledgment.** We thank Dr. A. Biswas and Prof. J. Blackwell for helpful discussions, in particular con-

cerning the comparison of the NMR and X-ray results. Financial support by the Bundesministerium für Forschung und Technologie, Projekt "Steife Makromoleküle" is gratefully acknowledged. It is a pleasure to thank Dr. N. Reynolds for his assistance in some of the experiments and Dr. J. Titman for his critical reading of the manuscript.

## References and Notes

- (1) Jackson, W. J., Jr. *Br. Polym. J.* **1980**, *12*, 154. Griffin, B. P.; Cox, M. K. *Br. Polym. J.* **1980**, *12*, 147.
- (2) Brüggling, W.; Kamschulte, U.; Schmidt, H. W.; Heitz, W. *Makromol. Chem.* **1988**, *189*, 2755.
- (3) Majnusz, J.; Catala, J. M.; Lenz, R. W. *Eur. Polym. J.* **1983**, *19*, 1043.
- (4) Ballauff, M. *Angew. Chem.* **1989**, *101*, 261.
- (5) Ballauff, M.; Schmidt, G. F. *Makromol. Chem. Rapid Commun.* **1987**, *8*, 93.
- (6) Biswas, A.; Deutscher, K.; Blackwell, J.; Wegner, G. *Macromolecules*, submitted for publication.
- (7) Whittaker, A. K.; Falk, U.; Spiess, H. W. *Makromol. Chem.* **1989**, *190*, 1603.
- (8) Baldwin Frech, C.; Adam, A.; Falk, U.; Boeffel, C.; Spiess, H. W. *New Polym. Mater.* **1990**, *2*, 267.
- (9) März, K. Ph.D. Thesis, University of Mainz, 1990.
- (10) Thürmer, A. Ph.D. Thesis, University of Mainz, 1992.
- (11) Spiess, H. W. *Chem. Rev.* **1991**, *91*, 1321.
- (12) Schmidt-Rohr, K.; Clauss, J.; Spiess, H. W. *Macromolecules* **1992**, *25*, 3237.
- (13) Schmidt-Rohr, K.; Clauss, J.; Blümich, B.; Spiess, H. W. *Magn. Reson. Chem.* **1990**, *28*, 3.
- (14) Adam, A.; Spiess, H. W. *Makromol. Chem., Rapid Commun.* **1990**, *11*, 249.
- (15) Ballauff, M. Private communication.
- (16) Dixon, W. T. *J. Chem. Phys.* **1982**, *77*, 1800.
- (17) Egger, N.; Schmidt-Rohr, K.; Blümich, B.; Domke, W. D.; Stapp, B. *J. Appl. Polym. Sci.* **1992**, *44*, 289.
- (18) Bovey, F. A. *Chain Structure and Conformation of Macromolecules*; Academic Press: New York, 1982.
- (19) Möller, M. *Adv. Polym. Sci.* **1985**, *66*, 59.
- (20) Wenzel, M.; Ballauff, M.; Wegner, G. *Makromol. Chem.* **1987**, *188*, 2865.
- (21) VanderHart, D. L.; Khoury, F. *Polymer* **1984**, *25*, 1589.
- (22) Ballauff, M.; Schmidt, G. F. *Mol. Cryst. Liq. Cryst.* **1987**, *147*, 163.
- (23) Biswas, A.; Schürmann, B. L. *Polym. Prepr. (Am. Chem. Soc., Div. Polym. Chem.)* **1992**, *33* (1), 562.
- (24) Biswas, A.; Schürmann, B. L. *J. Chem. Phys.* **1991**, *95*, 5377.
- (25) Biswas, A.; Schürmann, B. L. Private communication.
- (26) Adam, A.; Falk, U.; Boeffel, C.; Spiess, H. W. Manuscript in preparation.
- (27) Blackwell, J.; Biswas, A. In *Development in Oriented Polymers-2*; Ward, I. M., Ed.; Elsevier Applied Science: Dordrecht, The Netherlands, 1987; Chapter 5, p 153.

**Registry No.** 1 (copolymer), 107502-85-2; 1 (SRU), 103728-28-5; 2 (copolymer), 107502-77-2; 2 (SRU), 107502-98-7; 3 (copolymer), 132720-84-4; 3 (SRU), 112231-33-1.